Bioorganic & Medicinal Chemistry 19 (2011) 1426–1433

Contents lists available at ScienceDirect

Bioorganic & Medicinal Chemistry

journal homepage: www.elsevier.com/locate/bmc

Structure–activity relations on [1-(3,5-difluoro-4-hydroxyphenyl)-1*H*-pyrrol-3-yl]phenylmethanone. The effect of methoxy substitution on aldose reductase inhibitory activity and selectivity

Maria Chatzopoulou [a], Eduard Mamadou [a], Maria Juskova [b], Cathrine Koukoulitsa [c], Ioannis Nicolaou [a,*], Milan Stefek [b], Vassilis J. Demopoulos [a,*]

[a] Department of Pharmaceutical Chemistry, School of Pharmacy, Aristotle University of Thessaloniki, 54124 Thessaloniki, Greece
[b] Institute of Experimental Pharmacology and Toxicology, Slovak Academy of Sciences, Dubravska cesta 9, 841 04 Bratislava, Slovakia
[c] Department of Chemistry, University of Athens, 15784 Zographou, Greece

ARTICLE INFO

Article history:
Received 21 October 2010
Revised 29 December 2010
Accepted 5 January 2011
Available online 11 January 2011

Keywords:
Aldose and aldehyde reductase
ARI
Long-term diabetic complications
Sorbitol assay
Docking

ABSTRACT

Based on our previous work, we studied the effect of methoxy-substitution as well as the regioposition of the benzoyl-moiety of **4a** [(1-(3,5-difluoro-4-hydroxyphenyl)-1*H*-pyrrol-3-yl)(phenyl)methanone]. On this basis, compounds **4b–c** and **5a–c** were synthesized and assayed for aldose and aldehyde reductase inhibitory activity. Furthermore, a 4,6-difluoro-5-hydroxyphenyl pattern (**9**) was studied, in order to verify the optimum position of the phenol-moiety. Compound **5b** emerged as the most potent and selective inhibitor. Moreover, further assays proved **5b** as a potent antioxidant and an inhibitor of sorbitol accumulation in isolated rat lenses. Combining the above attributes, **5b** could serve as a lead compound targeted at long-term diabetes complications.

1. Introduction

Diabetes mellitus is a complex metabolic disorder affecting 285 million adults in 2010 and this number is estimated to increase to 439 million by 2030.[1] The increase in numbers is considered as a result of the dominant lifestyle that encourages low physical activity and the emergence of obesity, leading this disease to epidemic proportions. The high morbidity and mortality of diabetes (3.96 million in 2010[2]) is attributed to diabetes' chronic complications that develop over the years due to poor glycemic control. Macroangiopathies such as coronary artery disease, peripheral vascular and cerebrovascular disease are the main causes behind the high lethality of diabetes, accompanied by microangiopathies such as retinopathy, neuropathy and nephropathy that significantly lower the quality of the diabetic's life. Thus, it becomes clear that diabetes consists one of the major health problems worldwide, with the addition of a significantly high economic burden. According to recent statistical analyses in the US, 116 million dollars were spent on medical expenditures for diabetes during 2007, with 50% of this amount spent on the treatment of diabetes complications. Moreover, if the indirect costs (reduced productivity, disability, early mortality) are included the above amount is raised to 174 million dollars.[3]

Hyperglycemia, as a result of the instability in glucose regulation in the diabetic individual, is considered as the causative link on the onset and progression of diabetes chronic complications. Under hyperglycemic conditions, and especially in cells where the intake of glucose is non insulin-dependent, there is observed activation of the polyol pathway as a means to metabolize the glucose excess. This increased flux through the polyol pathway reaches up to 30% of the total glucose turnover.[4] As a consequence, osmotic, oxidative, reductive, glycative and protein kinase C (PKC) stress are induced[5] with devastating manifestations for the cells.

The polyol pathway was first linked to secondary complications of diabetes in the mid '60s.[6] Aldose reductase (ALR2, AR, E.C. 1.1.1.21, AKR1B1) is the first and rate-limiting enzyme of the polyol pathway, reducing glucose to sorbitol using NADPH as cofactor. Sorbitol is further metabolized to fructose by sorbitol dehydrogenase (SDH). In the investigations on the significance of these two enzymes and their implication on diabetes long-term complications, inhibition of ALR2 emerged as a novel pharmacotherapeutic target and the development of inhibitors (ARIs) has

Abbreviations: AKR, aldoketoreductase; ALR1, aldehyde reductase; ALR2, aldose reductase; ARI, aldose reductase inhibitor; PKC, protein kinase C; rmsd, root-mean squared deviation; SDH, sorbitol dehydrogenase.

* Corresponding authors. Tel.: +30 2310 998670; fax: +30 2310 997852 (I.N.); tel.: +30 2310 997626; fax: +30 2310 997852 (V.J.D.).
E-mail addresses: inikolao@pharm.auth.gr (I. Nicolaou), vdem@pharm.auth.gr (V.J. Demopoulos).

0968-0896/$ - see front matter © 2011 Elsevier Ltd. All rights reserved.
doi:10.1016/j.bmc.2011.01.009

been gaining attention since then. The most studied classes of inhibitors though, namely carboxylic acids and hydantoins, proved to have poor bioavailability or manifest adverse side effects.[7] As such, novel and selective chemotypes are sought in order to improve the therapeutic potential of ARIs and explore their clinical usage.

We have previously reported that in a series of benzoylpyrrol-1-ylacetic acids the introduction of the methoxy group in the benzoyl side group generally increases the activity.[8] Also, based on bioisosteric replacement of the acetic acid moiety with a 2,6-difluorophenol ring, compound **4a**, previously synthesized, proved to be a potent and selective ARI.[9,10] Thus, in order to investigate the effect of phenol position on activity and selectivity, compound **9** (Scheme 2) was synthesized. Since **4a** proved to be a more effective and selective inhibitor of ALR2, in contrast to **9**, we further processed on **4a** in order to delineate the effect of methoxy-substitution. On this basis, compounds **4b–c** and **5a–c** (Scheme 1) were synthesized and evaluated for ALR2 inhibitory activity. Furthermore, the selectivity index of the newly synthesized pyrrolyldifluorophenol derivatives towards the closely related enzyme aldehyde reductase (ALR1, E.C. 1.1.1.2, AKR1A1) was determined. Docking simulations were performed in order to examine the differences in activity and selectivity among the most intriguing derivatives. Finally, the antioxidant potential of the most active and selective compound **5b**, as well as its inhibition of sorbitol accumulation in isolated rat lenses was assessed.

2. Results and discussion

2.1. Chemistry

The synthesis of the target compounds **4a–c** and **5a–c** was achieved as described in Scheme 1. Friedel–Crafts aroylation of the respective aryl substituted 2,6-difluoro-4-pyrrol-1-yl-phenyl esters **3a–c**, was followed by alkaline hydrolysis of the crude formed intermediates. Based on a previous work on the regioselective synthesis of aroyl-pyrroles,[11] two methodologies were applied, varying on the Lewis acid catalysts. $AlCl_3$ and $BF_3{\cdot}Et_2O$ were utilized, producing various ratios among the isomeric products (see Table 1 for details). The results obtained are in accordance with those of Kakushima et al.,[11] though it should be underlined that the reactions in their work were highly regiospecific. Generally in our work, $AlCl_3$ as a catalyst directed mostly to the 3-isomer, whereas $BF_3{\cdot}Et_2O$ to the 2-isomer. It should also be mentioned, that aroylation of **3c** with both catalysts derived mostly the 3-isomer probably due to stereochemical reasons. Aroylation with $AlCl_3$ led to the massive production of the 3-isomer up to a percentage of 70%, whereas aroylation with $BF_3{\cdot}Et_2O$ led to the production of both isomers in a ratio close to 1:1 (52% and 44%).

Table 1
Friedel–Crafts aroylation yields with $AlCl_3$ and $BF_3{\cdot}Et_2O$

Compound	Yields	
	$AlCl_3$ (%)	$BF_3{\cdot}Et_2O$ (%)
4a	52	24
5a	36	50
4b	26	22
5b	36	49
4c	73	52
5c	10	44

Compound **9** was synthesized, as depicted in Scheme 2. The first step involved the reaction of 1,3-difluoro-4-iodo-2-methoxybenzene[12] (**6**) in a modified Ullman type coupling reaction with 3-benzoylpyrrole (**7**). In this modification, previously used for coupling reactions on a number of substituted pyrroles,[13] CuI and *trans-N,N′*-dimethylcyclohexane-1,2-diamine were used as catalysts and K_3PO_4 as the base. The desired product was derived upon deprotection of the methoxy-group with HBr cleavage.[12]

2.2. In vitro results

2.2.1. ALR2 inhibitory activity

ALR2 inhibitory activity was evaluated on partially purified rat lens ALR2. Human ALR2 exhibits 85% sequence homology to rat ALR2,[14] while the catalytic active sites of both enzymes are considered identical.[15] ALR2 inhibitory activity is expressed as IC_{50} values (Table 2). All the compounds exhibited inhibitory activities in the micromolar or submicromolar range. Changing the position of the phenol group (compound **9**) resulted in the maintenance of the inhibitory activity, although with a slight decrease in its magnitude. Furthermore, from the results obtained, it is deduced that the methoxy-substitution generally conserves the inhibitory activity, with the exception of compound **4b** in which activity decreases but is not totally eliminated. On the role of the position of the pyrrol-substitution no definite results could be drawn, since the most active compounds, **4a** and **5b**, are a β-substituted and a α-substituted pyrrole derivative, respectively. However, the α-substituted pyrrolyl methoxy derivatives (**5b**, **5c**) were more active compared to the respective β-substituted (**4b**, **4c**). In this respect, it is interesting to mention that in a lowest energy conformation[16] of **4b** and **4c** the intramolecular distance between the phenolic oxygen and methoxy oxygen is close to 14 Å, whereas in **5b** and **5c** is close to 11 Å.

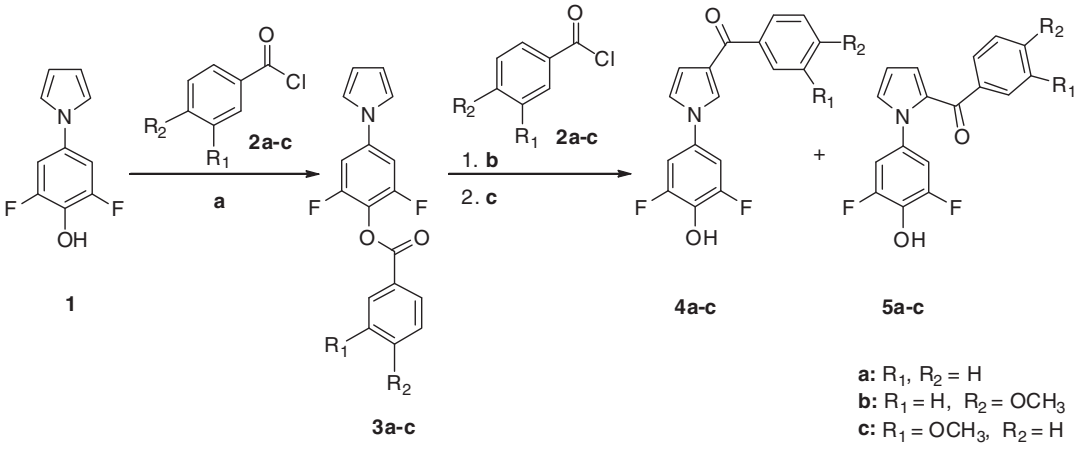

Scheme 1. Synthesis of compounds **4a–c** and **5a–c**. Reagents: (a) $(CH_3CH_2CH_2CH_2)_4N(HSO_4)$, NaOH, 1,4-dioxane; (b) $AlCl_3$ or $BF_3{\cdot}Et_2O$, CH_2Cl_2; (c)H_2O/NaOH, 1,4-dioxane.

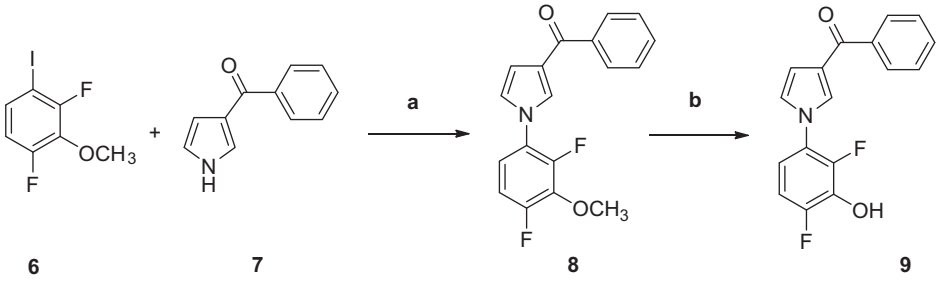

Scheme 2. Synthesis of compound **9**. Reagents: (a) *trans-N,N′*-dimethylcyclohexane-1,2-diamine, CuI, K_3PO_4, toluene; (b) aqueous 48% HBr/CH_3COOH.

Table 2
Aldose and aldehyde reductase inhibitory activity

Compound	IC_{50} ± SEM[a] (μM)		Selectivity index[b]
	Rat lens ALR2	Rat kidney ALR1	
4a	0.40 ± 0.02	13.4 ± 0.58	33.8
4b	24.9 ± 0.08	>100	>4
4c	9.93 ± 0.49	51.8 ± 1.00	5.2
5a	1.06 ± 0.16	4.6 ± 0.17	4.3
5b	0.39 ± 0.02	27.8 ± 5.10	71.6
5c	1.18 ± 0.04	23.5 ± 3.80	19.9
9	1.26 ± 0.02	1.61 ± 0.01	1.3
Sorbinil	0.25 ± 0.01[c]		
Valproic acid		56.1 ± 2.7[d]	

[a] $n = 3$.
[b] Defined as IC_{50} [ALR1]:IC_{50} [ALR2].
[c] Reported by Alexiou et al.[17]
[d] Reported by Pegklidou et al.[18] and Stefek et al.[19]

2.2.2. ALR1 inhibitory activity

ALR2 belongs to the aldoketoreductase (AKR) superfamily of enzymes. Among its many members, ALR2 shares the highest degree of similarity with ALR1. The two enzymes exhibit 65% sequence homology, as well as structural homology.[20] Since the closely related AKRs are related with the detoxification of toxic aldehydes,[21] parallel inhibition could cause unwanted effects. ALR1 inhibitory activity was evaluated on partially purified rat kidney enzyme and is expressed as IC_{50} values presented together with the calculated selectivity index (Table 2). From the obtained results it becomes clear that the methoxy derivatives are less active on ALR1 in comparison to their activity on ALR2. Furthermore, the β-substituted pyrrole derivatives (**4a–c**) are less active from their respective α-substituted analogues (**5a–c**) on ALR1. Regarding the selectivity index, no selectivity was observed when the phenol group was relocated (compound **9**). By far the most selective inhibitor was compound **5b**, which is also the most active ARL2 inhibitor.

2.2.3. Antioxidant capacity

Oxidative stress induced by hyperglycemia in diabetes mellitus has been highly interrelated in the emergence and progression of long-term diabetes complications.[19] The formation of reactive aldehydes, as well as oxidized glutathione (GSSG) are known products of such conditions that are also substrates for ALR2.[22] Furthermore, GSSG has been blamed for oxidation of ALR2 on key cysteine residues (Cys298) resulting in an oxidized form of the enzyme that has lower sensitivity to ARIs along with an increase in the affinity for aldehyde substrates.[23,24] Thus, the putative antioxidant activity of an ARI could account synergistically on the overall effectiveness of a pharmacotherapeutic agent targeted at diabetic chronic complications, both by preventing the enzyme's oxidation and by reacting with the highly reactive oxidants produced during hyperglycemia. The antioxidant inhibitory efficiency of **5b** was evaluated in the heterogenous system of unilamellar L-α-phosphatidylcholine dioleoyl (DOPC) liposomes. DOPC were used as model membranes oxidatively stressed by peroxy radicals generated in the aqueous phase by thermal decomposition of the hydrophilic azo-initiator 2,2′-azobis(2-amidinopropane)hydro-chloride (AAPH). In this system factors such as membrane permeability as well as location of the antioxidant and radical rigidly affect the antioxidant reactivity. Compound **5b** was found to inhibit peroxidation of DOPC liposomes more efficiently than the known antioxidant trolox (IC_{50} = 35.77 and 93.5[18,19] μM for **5b** and trolox, respectively).

2.2.4. Inhibitory activity on rat lens sorbitol accumulation

Increased ALR2 activity as well as elevated sorbitol levels have been recently reported in type II diabetes patients with diabetic retinopathy.[25] Of the stress-hypotheses mentioned earlier, osmotic stress caused by sorbitol accumulation has been shown to be of utmost importance in the diabetic's lens, leading eventually to cataract formation.[26] On this basis, we studied the effect of the most active compound **5b** on glucose-induced sorbitol accumulation at an organ level in the rat lens cultivated in the presence of high glucose in vitro. As shown in Table 3, significantly increased sorbitol levels were recorded in the lenses incubated with glucose in comparison with control incubations without glucose, reflecting increased flux through ALR2. Similarly, other authors[27] observed more than 10-fold increase of sorbitol level in the eye lenses incubated with glucose under comparable conditions (50 mM glucose, 4 h incubation). Sorbitol production was significantly inhibited by compound **5b** with efficacy comparable to that of equimolar tetramethylene glutaric acid (TMGA). The latter is a specific inhibitor of ALR2, used also by other authors at the cellular level of isolated red blood cells.[28–30]

3. Computational methods

The structure of ALR2 active site has been extensively analyzed by both crystallographic and modeling studies. It has proved to be highly hydrophobic in nature and is formed by aromatic residues (Trp20, Tyr48, Trp79, Trp111, Phe121, Phe122 and Trp219), apolar residues (Val47, Pro218, Leu300 and Leu301), and polar residues (Gln49, Cys298 and His110). The nicotinamide ring of $NADP^+$ is

Table 3
Effect of compound **5b** on sorbitol accumulation in isolated rat lenses cultivated with high glucose in comparison with standard TMGA

Incubation	Sorbitol (nmol/g)	*n*
−Glucose[a]	39.6 ± 10.3	3
+Glucose	643.5 ± 133.0	11
+Glucose + **5b** (100 μM)	203.5 ± 42.9[b]	6
+Glucose + TMGA[c] (100 μM)	205.8 ± 30.5[b]	3

Results are mean values ± SD from *n* independent incubations.
[a] Glucose, 50 mM; time of incubation, 3 h; 37 °C.
[b] $p < 0.001$ versus +Glucose.
[c] TMGA = tetramethylene glutaric acid.

centered in the cavity and the three possible proton donors responsible for catalysis are Tyr48, His110 and Trp111 all composing the anionic binding pocket.[5,31,32] Inhibitor selectivity remains an issue to consider, since the corresponding residues in the ALR1 active site are highly conserved (Tyr50, His113 and Trp114).[33] The difference in inhibitor potency for the two enzymes has been attributed to non-conserved residues located in the C-terminal loop lining a hydrophobic region of the active site called the 'specificity pocket'.[33] This pocket binds inhibitors that are more effective against ALR2 than against ALR1.[34]

Docking simulations of the most intriguing compounds were performed in order to shed light on their interactions in the active site of ALR2. The human ALR2 holoenzyme cocrystallized with IDD 594 (PDB entry 1US0) was selected, as it was determined at the highest resolution (0.66 Å) among all the available structures. The X-ray crystallography study revealed that the inhibitor IDD 594 induces a conformational change upon binding to ALR2, creating a specificity pocket localized between Phe122, Trp111, Leu300, and Ala299. The carboxylate group is firmly anchored in the active site with hydrogen bonds to His110, Tyr48, and Trp111 and with a strong electrostatic interaction with $NADP^+$.

The docking simulations were performed by the docking GLUE program, which has been shown to successfully reproduce experimentally observed binding modes in terms of rmsd (root-mean squared deviation). The crystallographic structure of IDD 594 was docked into ALR2 with GLUE provided excellent results as shown in our previous work.[35]

Docking calculations showed that the most active compound (**5b**) exhibits the lower binding energy (−28.32 kcal/mol). As illustrated in Figure 1a, the compound was placed in the same location as IDD 594 in the crystal structure. In particular, compound **5b** is anchored in the anionic binding site forming a polar interaction between the carbonyl oxygen and Trp111, and electrostatic interactions with the positively charged nicotinamide ring of $NADP^+$. A hydrogen bond is also formed between the hydrogen of the hydroxyl group of the 3,5-difluorophenol ring and the oxygen of Thr113. Further stabilization of the molecule is attributed to the aromatic interactions of the phenyl rings with Trp20, Trp79, Trp111, and Van der Waals interactions between phenyl rings and residues Phe122, and Leu300. It should be noticed that the phenyl ring entered in the specificity pocket localized between Phe122, Trp111, Leu300, and Ala299, as IDD 594, suggesting a selectivity for ALR2 versus ALR1 (Fig. 1b). This is in accordance with the experimental result regarding the selectivity index (Table 2), which indicates that compound **5b** is by far the most selective inhibitor. Docking calculations in the active site of ALR1 were performed in order to compare the interactions of inhibitor **5b** in the two enzymes. The porcine ALR1 holoenzyme cocrystallized with the potent aldose reductase inhibitor Fidarestat (PDB entry 3H4G) was selected.[33] In both enzymes Fidarestat is anchored through its cyclic imide ring to the active site and the hydrogen-bonding network with the active-site residues Tyr50, His, 113, and Trp114 is conserved. Docking simulations of compound **5b** (−11.77 kcal/mol) in the active site of ALR1, showed that it cannot establish strong interactions with the key aminoacids of the active site and $NADP^+$. In contrast, compound **9**, for which no selectivity was observed, exhibited lower binding energy (−14.43 kcal/mol) in comparison to inhibitor **5b** and showed polar interactions with the key aminoacids of ALR1 (Fig. 1d).

Compound **4a** possess similar binding energy (−27.55 kcal/mol), and as is depicted in Figure 2a is placed in the same location as IDD 594 and **5b**. The compound is oriented in the active site so that the fluorine atom at position 3 develops a hydrogen bond with His110 and polar interactions with Tyr48 and Trp111. The molecule is also stabilized forming polar interactions between the fluorine atom at position 5 and Trp20. A hydrogen bond is also formed between the hydrogen of the hydroxyl group and the nitrogen of Trp20. Compound **4b** entered the anionic binding site with the 4-methoxy phenyl ring forming a polar interaction between the carbonyl oxygen and the nitrogen of Trp111 (Fig. 2b). It exhibits the higher binding energy (−22.78 kcal/mol) among the studied compounds and this result is consistent with the observed reduced inhibitory activity of compound **4b** against ALR2.

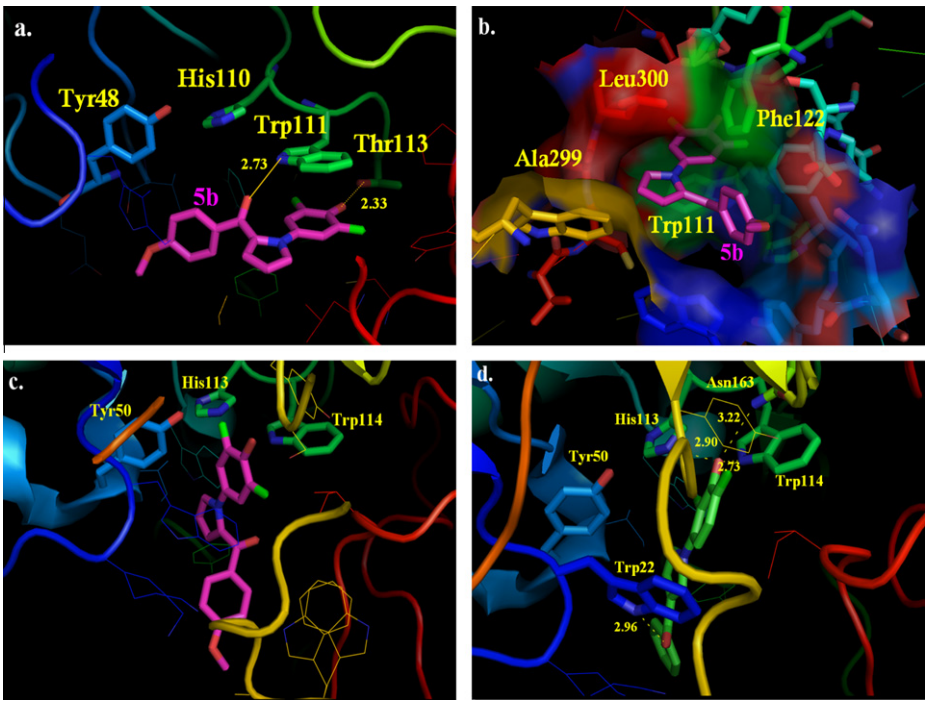

Figure 1. Docked orientations of (a) compound **5b** with additional depiction of the key aminoacids of ALR2 active site. Polar interactions and hydrogen bonds are shown as dotted lines; (b) compound **5b** in the specificity pocket; (c) compound **5b** with additional depiction of the key aminoacids of ALR1 active site; (d) compound **9** with additional depiction of the key aminoacids of ALR1 active site. Polar interactions and hydrogen bonds are shown as dotted lines.

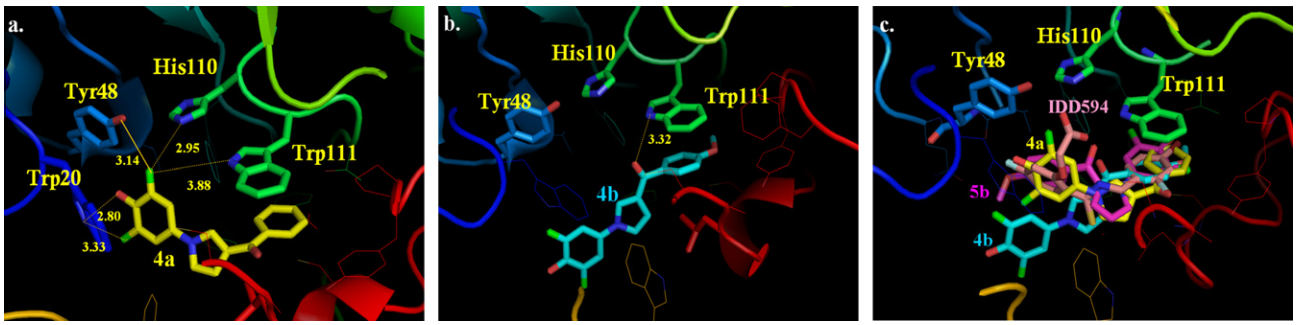

Figure 2. (a) Compound **4a**, and (b) compound **4b**, with additional depiction of the key aminoacids of ALR2 active site. Polar interactions and hydrogen bonds are shown as dotted lines; (c) superimposition of the docked compounds **5b**, **4a**, and **4b** and IDD594 in the active site of ALR2.

In Figure 2c is presented the superimposition of the docked compounds and IDD594 in the active site of ALR2.

4. Conclusions

To the previously synthesized **4a** we studied the effect of the phenol position and since **4a** proved to be more active and selective than **9**, we further proceeded to examine the effect of methoxy-substitution on the benzoyl-moiety on **4a**, as well as the position of the aroyl-substitution on the pyrrolyl-ring. The newly synthesized methoxy derivatives (**4b–c**, **5b–c**) retained micromolar inhibitory activities for ALR2 enzyme and furthermore α-substituted pyrroles (**5b–c**) shown greater selectivity towards the homologous enzyme ALR1. The most active compound **5b** exhibited submicromolar inhibitory activity towards ALR2 and was highly selective [selectivity index = 72]. These results are in accordance with docking simulations performed on the most intriguing compounds and ALR2 and ALR1 enzymes. **5b** was further assessed for its antioxidant capacity on the DOPC liposomes model and found to be a more potent antioxidant than trolox. Moreover, on a model of isolated rat lenses, **5b** inhibited sorbitol accumulation to an extend similar of the known ARI TMGA. Considering the above attributes, **5b** could be considered as a lead compound for further development in the field of novel inhibitors that combine ALR2 inhibitory activity and selectivity, potent antioxidant capacity and furthermore inhibition of sorbitol accumulation, attributes that are of key importance in the pathology of diabetes chronic complications.

5. Experimental section

5.1. General notes

All reagents were purchased from Sigma–Aldrich Co. and used without further purification. IR spectra were taken with a double beam spectrometer Hitachi U-2001. ^{1}H NMR spectra were recorded on a Bruker AW80 80 MHz with internal TMS standard. Melting points are uncorrected and were determined in open glass capillaries using a Mel-Temp II apparatus. Flash column chromatography was carried out with Merck Silica Gel 60 (230–400 Mesh ASTM). TLC was run with Fluka Silica gel/TLC-cards. Elemental analyses were performed by Perkin–Elmer 2400 CHN analyzer and the results are within ±0.4% of the theoretical values.

5.2. Chemistry

5.2.1. General procedure A. Preparation of the 2,6-difluoro-4-pyrrol-1-yl-phenol esters (3a–c)

To a mixture of 2,6-difluoro-4-pyrrol-1-yl-phenol[9] (**1**) (0.975 g, 5 mmol), tetrabutylammonium hydrogen sulfate (0.1 g, 0.3 mmol) and NaOH powder (0.5 g) in 1,4-dioxane (12.5 mL) under a nitrogen atmosphere, a solution of the appropriate aroyl chloride (**2a–c**) (7 mmol) in 1,4-dioxane (5 mL) was added dropwise for 30 min. The mixture was filtered, washed with 1,4-dioxane (3 × 10 mL) and evaporated under reduced pressure. The residue was flashed chromatographed with a suitable mixture of petroleum ether/EtOAc. Analytical samples were obtained by recrystallization from CH_2Cl_2/petroleum ether.

5.2.1.1. 2,6-Difluoro-4-(1*H*-pyrrol-1-yl)phenyl benzoate (3a). Prepared as described by Nicolaou et al.[9]

5.2.1.2. 2,6-Difluoro-4-(1*H*-pyrrol-1-yl)phenyl 4-methoxybenzoate (3b). Prepared from 4-methoxybenzoyl chloride according to the general procedure A (1.251 g, 77%). Mp 152–153 °C; IR (nujol) 1740 cm^{-1}; ^{1}H NMR ($CDCl_3$) δ 4.05 (s, 3H), 6.30–6.50 (m, 2H), 6.95–7.30 (m, 6H), 8.10–8.30 (m, 2H). Anal. Calcd for $C_{18}H_{13}F_2NO_3{\cdot}0.05CH_2Cl_2$: C, 65.00; H, 3.96; N, 4.20. Found: C, 64.82; H, 3.59; N, 4.16.

5.2.1.3. 2,6-Difluoro-4-(1*H*-pyrrol-1-yl)phenyl 3-methoxybenzoate (3c). Prepared from 3-methoxybenzoyl chloride according to the general procedure A (1.307 g, 80%). Mp 147–148 °C; IR (nujol) 1748 cm^{-1}; ^{1}H NMR ($CDCl_3$) δ 3.90 (s, 3H), 6.30–6.50 (m, 2H), 7.00–7.60 (m, 6H), 7.65–8.00 (m, 2H). Anal. Calcd for $C_{18}H_{13}F_2NO_3$: C, 65.65; H, 3.98; N, 4.25. Found: C, 65.45; H, 4.05; N, 4.24.

5.2.2. General procedure B. Friedel–Crafts aroylation with $AlCl_3$ as Lewis acid. Preparation of(1-(3,5-difluoro-4-hydroxyphenyl)-1*H*-pyrrol-yl)(aroyl)methanones (4a–c, 5a–c)

In a mixture of anhydrous $AlCl_3$ (6 mmol) in CH_2Cl_2 (10 mL) the appropriate aroyl chloride (5.6 mmol) was added slowly and stirred at room temperature and under a nitrogen atmosphere. After 10 min, a solution of the substituted ester of an aromatic acid with 2,6-difluoro-4-pyrrol-1-yl-phenol (5 mmol) (**3a–c**) in CH_2Cl_2 (5 mL) was added and the resulting mixture was stirred for 3 h under a nitrogen atmosphere. The reaction was quenched with ice and water and the product was extracted with CH_2Cl_2 (2 × 20 mL). The combined organic extracts were washed with saturated NaCl solution, dried over anhydrous Na_2SO_4, and evaporated under reduced pressure. The residue was dissolved in 1,4-dioxane (20 mL) and to this a solution of aqueous 5% NaOH solution (20 mL) was added. The mixture was stirred at room temperature and monitored for the hydrolysis of the ester group by TLC. When the reaction ended, the mixture was concentrated to half of its volume, H_2O (50 mL) was added, and it was cooled (ice bath) and acidified with concentrated HCl. Afterwards, the mixture was extracted with EtOAc (2 × 50 mL) and the combined organic extracts were washed with saturated NaCl solution, dried over Na_2SO_4, and the solvents were evaporated under reduced pressure.

In the residue, H_2O (50 mL) was added and it was alkalized with Et_3N. Afterwards, the mixture was extracted with AcOEt (2 × 50 mL) and dried over anhydrous Na_2SO_4. The solvents were evaporated under reduced pressure and the residue was flash chromatographed with petroleum ether/EtOAc (10:1–10:2) in order to purify both α and β products. Analytical samples were obtained by recrystallization from toluene/petroleum ether to provide the desired products.

5.2.2.1. (1-(3,5-Difluoro-4-hydroxyphenyl)-1*H*-pyrrol-3-yl)(phenyl)methanone (4a). Prepared from **3a** according to general procedure B (778 mg, 52%). Analytical data can be found by Nicolaou et al.[9]

5.2.2.2. (1-(3,5-Difluoro-4-hydroxyphenyl)-1*H*-pyrrol-2-yl)(phenyl)methanone (5a). Prepared from **3a** according to the general procedure B (593 mg, 36%). Mp 168–169 °C; IR (nujol) 3100, 1602 cm^{-1}; ^1H NMR ($CDCl_3$) δ 6.20–6.40 (m, 1H), 6.80–7.10 (m, 4H), 7.40–7.60 (m, 4H), 7.75–7.95 (m, 2H). Anal. Calcd for $C_{17}H_{11}F_2NO_2$: C, 68.23; H, 3.70; N, 4.68. Found: C, 68.03; H, 3.79; N, 4.59.

5.2.2.3. (1-(3,5-Difluoro-4-hydroxyphenyl)-1*H*-pyrrol-3-yl)(4-methoxyphenyl)methanone (4b). Prepared from **3b** according to the general procedure B (428 mg, 26%). Mp 214–215 °C; IR (nujol) 3111, 1611 cm^{-1}; ^1H NMR ($CDCl_3$/DMSO-d_6) δ 4.00 (s, 3H), 6.65–6.80 (m, 1H), 6.90–7.35 (m, 6H), 7.60–7.75 (br s, 1H), 7.80–8.05 (m, 2H). Anal. Calcd for $C_{18}H_{13}F_2NO_3$: C, 65.65; H, 3.98; N, 4.25. Found: C, 65.74; H, 3.99; N, 4.09.

5.2.2.4. (1-(3,5-Difluoro-4-hydroxyphenyl)-1*H*-pyrrol-2-yl)(4-methoxyphenyl)methanone (5b). Prepared from **3b** according to the general procedure B (593 mg, 36%). Mp 185–186 °C; IR (nujol) 3100, 1611–1586 cm^{-1}; ^1H NMR ($CDCl_3$/DMSO-d_6) δ 3.85 (s, 3H), 6.20–6.40 (m, 1H), 6.70–7.15 (m, 7H), 7.75–8.00 (m, 2H). Anal. Calcd for $C_{18}H_{13}F_2NO_3$: C, 65.65; H, 3.98; N, 4.25. Found: C, 65.29; H, 3.70; N, 4.18.

5.2.2.5. (1-(3,5-Difluoro-4-hydroxyphenyl)-1*H*-pyrrol-3-yl)(3-methoxyphenyl)methanone (4c). Prepared from **3c** according to the general procedure B (1202 mg, 73%). Mp 119–120 °C; IR (nujol) 3100, 1625 cm^{-1}; ^1H NMR ($CDCl_3$/DMSO-d_6) δ 3.80 (s, 3H), 6.65–6.80 (m, 1H), 6.80–7.20 (m, 5H), 7.25–7.55 (m, 4H). Anal. Calcd for $C_{18}H_{13}F_2NO_3$: C, 65.65; H, 3.98; N, 4.25. Found: C, 65.36; H, 3.72; N, 4.36.

5.2.2.6. (1-(3,5-Difluoro-4-hydroxyphenyl)-1*H*-pyrrol-2-yl)(3-methoxyphenyl)methanone (5c). Prepared from **3c** according to the general procedure B (165 mg, 10%). Mp 129–130 °C; IR (nujol) 3260, 1620 cm^{-1}; ^1H NMR ($CDCl_3$/DMSO-d_6) δ 3.80 (s, 3H), 6.20–6.40 (m, 1H), 6.80–7.60 (m, 9H). Anal. Calcd for $C_{18}H_{13}F_2NO_3$: C, 65.65; H, 3.98; N, 4.25. Found: C, 65.46; H, 4.01; N, 4.19.

5.2.3. General procedure C. Friedel–Crafts aroylation with BF_3·Et_2O as Lewis acid. Preparation of (1-(3,5-difluoro-4-hydroxyphenyl)-1*H*-pyrrolyl)(aroyl)methanones (4a–c, 5a–c)

In a mixture of BF_3·Et_2O (28 mmol) in CH_2Cl_2 (100 mL), the appropriate aroyl chloride (28 mmol) was added slowly and stirred at room temperature and under a nitrogen atmosphere. After 10 min, a solution of the substituted ester of an aromatic acid with 2,6-difluoro-4-pyrrol-1-yl-phenol (5,5 mmol) (**3a–c**) in CH_2Cl_2 (5 mL) was added and the resulting mixture was stirred for 72 h under a nitrogen atmosphere. The reaction was quenched with ice and water and the product was extracted with CH_2Cl_2 (2 × 20 mL). The combined organic extracts were washed with saturated NaCl solution, dried over anhydrous Na_2SO_4, and evaporated under reduced pressure. Hydrolysis and purification proceeded as described above in general procedure B.

5.2.3.1. (1-(3,5-Difluoro-4-hydroxyphenyl)-1*H*-pyrrol-3-yl)(phenyl)methanone (4a). Prepared from **3a** according to general procedure C (395 mg, 24%).

5.2.3.2. (1-(3,5-Difluoro-4-hydroxyphenyl)-1*H*-pyrrol-2-yl)(phenyl)methanone (5a). Prepared from **3a** according to the general procedure C (823 mg, 50%).

5.2.3.3. (1-(3,5-Difluoro-4-hydroxyphenyl)-1*H*-pyrrol-3-yl)(4-methoxyphenyl)methanone (4b). Prepared from **3b** according to the general procedure C (398 mg, 22%).

5.2.3.4. (1-(3,5-Difluoro-4-hydroxyphenyl)-1*H*-pyrrol-2-yl)(4-methoxyphenyl)methanone (5b). Prepared from **3b** according to the general procedure C (887 mg, 49%).

5.2.3.5. (1-(3,5-Difluoro-4-hydroxyphenyl)-1*H*-pyrrol-3-yl)(3-methoxyphenyl)methanone (4c). Prepared from **3c** according to the general procedure C (942 mg, 52%).

5.2.3.6. (1-(3,5-Difluoro-4-hydroxyphenyl)-1*H*-pyrrol-2-yl)(3-methoxyphenyl)methanone (5c). Prepared from **3c** according to the general procedure C (616 mg, 34%).

5.2.4. [1-(2,4-Difluoro-3-methoxyphenyl)-1*H*-pyrrol-3-yl]-phenylmethanone (8)

To a solution of **6**[12] (1 g, 3.7 mmol) in dry toluene (4 mL), **7**[36] (528 mg 3,08 mmol), *trans*-tetramethylcyclohexane-1,2-diamine (88 mg, 0.62 mmol), K_3PO_4 (1.373 g, 6.47 mmol) and CuI (29 mg, 0.15 mmol) were added and the mixture was refluxed under a nitrogen atmosphere for 24 h. The reaction mixture was cooled to room temperature; AcOEt (5 mL) was added, filtered through a plug of silica, eluted with additional EtOAc (30–50 mL) and the solvents were removed under reduced pressure. The resulting residue was purified by silica gel flash column chromatography (petroleum ether/AcOEt 10:1) to provide the title compound (833 mg, 86%) as a yellowish oil. IR (nujol) 1978 cm^{-1}; ^1H NMR ($CDCl_3$) δ 4.05 (s, 3H), 6.79–8.00 (m, 10H). Anal. Calcd for $C_{18}H_{13}F_2NO_2$·$0.02CH_2Cl_2$: C, 68.71; H, 4.17; N, 4.45. Found: C, 68.75; H, 4.00; N, 4.37.

5.2.5. [1-(2,4-Difluoro-3-hydroxyphenyl)-1*H*-pyrrol-3-yl]-phenylmethanone (9)

To a solution of **8** (200 g, 0.64 mmol) in glacial acetic acid (3.5 mL), an aqueous 48% HBr solution (3.5 mL) was added and the mixture was refluxed under a nitrogen atmosphere for 12 h. The reaction mixture was cooled to room temperature and the solvents were removed under reduced pressure. The resulting residue was flash chromatographed with petroleum ether/AcOEt (4:1) followed by recrystallization from CH_2Cl_2/petroleum ether to provide the title compound (89 mg, 46%). Mp: 139–142 °C; IR (nujol) 3113, 1612 cm^{-1}; ^1H NMR ($CDCl_3$/DMSO-d_6) δ 6.79–7.08 (m, 4H), 7.38–7.64 (m, 4H), 7.76–7.98 (m, 2H). Anal. Calcd for $C_{17}H_{11}F_2NO_2$·$0.15CH_2Cl_2$: C, 66.02; H, 3.65; N, 4.49. Found: C, 66.00; H, 3.50; N, 4.42.

5.3. Biological evaluation

5.3.1. ALR2 preparation

The target compounds **4b–c, 5a–c** and **9** were dissolved in 10% aqueous solution of $NaHCO_3$. Lenses were quickly removed from

Fischer-344 rats of both sexes following euthanasia. The experiments conform to the law for the protection of experimental animals (Republic of Greece) and are registered at the Veterinary Administration of the Republic of Greece. ALR2 from rat lens was partially purified according to the reported procedure[17–19] as follows: lenses were quickly removed from rats following euthanasia and stored at −20 °C until used. The lenses were homogenized in 5 vol of cold distilled water. The homogenate was centrifuged at 10,000*g* at 0–4 °C for 15 min. The supernatant was precipitated with saturated ammonium sulfate at 40% salt saturation and this solution was centrifuged at 10,000*g* at 0–4 °C for 15 min. The latter supernatant was either used directly or stored for maximum 24 h at −80 °C.

5.3.2. ALR1 preparation

The tested compounds **4a–c, 5a–c** and **9** were dissolved in 10% aqueous solution of $NaHCO_3$. Kidneys were quickly removed from Fischer-344 rats of both sexes following euthanasia. The experiments conform to the law for the protection of experimental animals (Republic of Greece) and are registered at the Veterinary Administration of the Republic of Greece. ALR1 from rat kidney was partially purified according to the reported procedure[18,37] as follows: kidneys were homogenized in a knife homogenizer followed by processing in a glass homogenizer with a teflon pestle in 3 vol of 10 mM sodium phosphate buffer, pH 7.2, containing 0.25 M sucrose, 2.0 mM EDTA dipotassium salt, and 2.5 mM β-mercaptoethanol. The homogenate was centrifuged at 10,000*g* at 0–4 °C for 30 min and the supernatant was subjected to ammonium sulfate fractional precipitation at 40%, 50%, and 75% salt saturation. The pellet obtained from the last step, possessing ALR1 activity, was redissolved in 10 mM sodium phosphate buffer, pH 7.2, containing 2.0 mM EDTA dipotassium salt and 2.0 mM β-mercaptoethanol to achieve total protein concentration of approx. 20 mg/mL. DEAE DE 52 resin was added to the solution (33 mg/mL) and after gentle mixing for 15 min removed by centrifugation. The supernatant containing ALR1 was then stored in smaller aliquots at −80 °C. No appreciable contamination by ALR2 in ALR1 preparations was detected since no activity in terms of NADPH consumption was observed in the presence of glucose substrate up to 150 mM.

5.3.3. Enzyme assays

ALR2 and ALR1 activities were assayed spectrophotometrically by determining NADPH consumption at 340 nm. In order to determine ALR2 inhibitory activity D,L-glyceraldehyde was used as a substrate and the measurements took place in 30 °C, whereas ALR1 inhibitory activity was determined with D-glycuronate as a substrate and the measurements took place in 37 °C. Compounds **4a–c, 5a–c** and **9** were tested at five concentrations, the log (dose)–response curves were then constructed from the inhibitory data, and the IC_{50} values were calculated by least-square analysis of the linear portion of the log (dose) versus response curves. The experiments were performed in triplicate.

5.3.4. DOPC liposome preparation, incubation and LOOH determination

The experimental protocol is based on a previously described methodology.[17,19,38,39] A suspension of unilamellar L-a-phosphatidylcholine dioleoyl (C18:1,[cis]-9; DOPC; 99% grade) liposomes (1 mM) in phosphate buffer (20 mL, 20 mM, pH 7.4) was prepared. The liposomes (final concentration 0.8 mM DOPC) were incubated in the presence of different concentrations of compound **5b** (10–300 μM) with the water-soluble initiator AAPH (final concentration 10 mM) at 50 °C for 80 min. Aliquots (1 mL) of the incubation mixtures were extracted with 2 mL portions of an ice-cold mixture of $CHCl_3$/MeOH (2:1, v/v) containing 2,6-di-*tert*-butyl-*p*-cresol (BHT) (0.05%). The lipid hydroperoxide content was determined by the thiocyanate method by sequentially adding the $CHCl_3$/MeOH (2:1, v/v) mixture (1.4 mL) and the thiocyanate reagent (0.1 mL).[40] The thiocyanate reagent was prepared by mixing equivalent volumes of a methanolic solution of KSCN (3%) and a ferrous ammonium sulfate solution (45 mM in 0.2 mM HCl). After the mixture had been left at ambient temperature for at least 5 min, the absorbance at 500 nm was recorded. The lipid peroxide value was determined using a calibration curve prepared with standard cumene hydroperoxide. The value of IC_{50} was obtained by least-square analysis of the linear part of the semi logarithmic plot of I (%, percentage of inhibition) versus antioxidant concentration ($0.936 < r^2 < 0.978$). The experiment was performed in triplicate.

5.3.5. Eye lenses sorbitol assay

Male Wistar rats, 8–9 weeks old, weighing 200–250 g, were used. The animals came from the Breeding Facility of the Institute of Experimental Pharmacology and Toxicology, Dobra Voda (Slovak Republic). The study was approved by the Ethics Committee of the Institute and performed in accordance with the Principles of Laboratory Animal Care (NIH publication 83–25, revised 1985) and the Slovak law regulating animal experiments (Decree 289, Part 139, July 9th 2003). The animals in light ether anesthesia were killed by exsanguinations of the carotid artery and the eye globes were excised. The lenses were quickly dissected and rinsed with ice-cold saline.

The compounds studied were added into the tubes containing freshly dissected eye lenses (1 lens per tube) in 10 mmol/l isotonic phosphate buffered saline (PBS, pH 7.4, 1.9 mM NaH_2PO_4, 8.1 mM Na_2HPO_4 and 150 mM NaCl)[41] bubbled at 37 °C with pneumoxid (5% CO_2, 95% O_2) to the final concentration of 100 μmol/L, 30 min before adding glucose. The incubation was initiated by adding glucose to the final concentration of 50 mmol/L and then continued at 37 °C with occasional (in about 30-min intervals) bubbling the mixture for approximately 30-s periods with pneumoxid. The incubations were terminated after a 3-h period by cooling the mixtures in an ice bath, followed by washing the lenses three times with ice-cold PBS (1 mL). The short term cultivations were preferred to avoid substantial permeability changes of the eye lenses. The washed lenses were kept deep-frozen for sorbitol determination.

To determine sorbitol, the frozen lenses were let to melt at the ambient temperature. Then distilled water (0.2 mL/1 lens) was added. The lenses were disrupted by a glass rod. The rod was washed twice with distilled water (0.1 mL) and the suspension was ultra-sounded for 5 min. Thereafter, ice-cold $HClO_4$ (9%, 0.4 mL) was added and mixed thoroughly. The mixture was ultra-sounded for another 5 min and then kept on ice for 30 min to let proteins precipitate. The precipitated protein was spun off (15 min at 3000 rpm) at 4 °C. The supernatant was neutralized with concentrated K_2CO_3 (4 mol/L).

The neutralized supernatant was used for determination of sorbitol concentration by modified enzymatic analysis according to Mylari et al.[42] Briefly, sorbitol was oxidized to fructose by SDH with concomitant reduction of resazurin by diaphorase to the highly fluorescent resorufin. The final concentrations of the assay solutions were: diaphorase (11.5 U/25 mL triethanolamine buffer), NAD^+ (25 mg/25 mL triethanolamine buffer), resazurin (25 μL of 2 mmol/L resazurin solution in 25 mL of triethanolamine buffer), SDH (15.025 U/L mL triethanolamine buffer). Reaction mixtures were incubated for 60 min at room temperature with an opaque cover. The sample fluorescence was determined at 544 nm excitation and 590 nm emission. After the appropriate blanks were subtracted from each sample, the amount of sorbitol in nmol/g of lens wet weight in each sample was determined by comparison with a linear regression of sorbitol standards.

5.4. Computational methods

The molecules were constructed using SPARTAN.[16] Energy minimization (AM1 method), followed by Monte-Carlo conformation analysis were applied in order to calculate the lowest energy conformations of the synthesized compounds. The X-ray structure of human aldose reductase holoenzyme (PDB 1US0), and of porcine aldehyde reductase holoenzyme (PDB 3H4G) was used in our docking calculations after deletion of the inhibitor IDD 594 and FID from the PDB files, respectively, obtained from the Brookhaven Protein Data Bank [RCSB Protein Data Bank, operated by the Research Collaboratory for Structural Bioinformatics]. Docking calculations were performed with GLUE[43] program implemented in the GRID package (www.moldiscovery.com).[44] GLUE is a docking procedure aimed at detecting energetically favourable binding modes of a ligand with respect to the protein active site using the GRID force field.[45] The protein cavity is mapped using several GRID runs: a set of different probes is used to mimic all chemical groups present in the ligand and the resulting maps are encoded into compact files which store the interaction energies. PyMol[46] molecular graphics system was used in order to visualize the results of the docking.

Acknowledgements

This work was financially supported by the Greek State Scholarship Foundation and Aristotle University's Research Comittee. Also, financial support by grants COST B35 and VEGA 2/0001/08 are gratefully acknowledged. Furthermore, the authors would like to thank Professor Gabriele Cruciani (Laboratory for Chemometrics, School of Chemistry, University of Perugia, Italy) for kindly providing us the GRID package. At last, many thanks to Dr. Polyxeni Alexiou for her help and advice on the experimental protocols.

References and notes

1. Shaw, J. E.; Sicree, R. A.; Zimmet, P. Z. *Diabetes Res. Clin. Pract.* **2010**, *87*, 4.
2. Roglic, G.; Unwin, N. *Diabetes Res. Clin. Pract.* **2010**, *87*, 15.
3. *Diabetes Care* **2008**, *31*, 596.
4. Demopoulos, V. J.; Zaher, N.; Zika, C.; Anagnostou, C.; Mamadou, E.; Alexiou, P.; Nicolaou, I. *Drug Des. Rev. Online* **2005**, *2*, 293.
5. Alexiou, P.; Pegklidou, K.; Chatzopoulou, M.; Nicolaou, I.; Demopoulos, V. J. *Curr. Med. Chem.* **2009**, *16*, 734.
6. Gabbay, K. H. *Ann. Rev. Med.* **1975**, *26*, 521.
7. Sturm, K.; Levstik, L.; Demopoulos, V. J.; Kristl, A. *Eur. J. Pharm. Sci.* **2006**, *28*, 128.
8. Nicolaou, I.; Demopoulos, V. J. *J. Med. Chem.* **2003**, *46*, 417.
9. Nicolaou, I.; Zika, C.; Demopoulos, V. J. *J. Med. Chem.* **2004**, *47*, 2706.
10. Papezikova, I.; Pekarova, M.; Chatzopoulou, M.; Nicolaou, I.; Demopoulos, V. J.; Kubala, L. *Neuroendocrinol. Lett.* **2008**, *29*, 775.
11. Kakushima, M.; Hamel, P.; Frenette, R.; Rokach, J. *J. Org. Chem.* **1983**, *48*, 3214.
12. Qiu, J.; Stevenson, S. H.; O'Beirne, M. J.; Silverman, R. B. *J. Med. Chem.* **1999**, *42*, 329.
13. Antilla, J. C.; Baskin, J. M.; Barder, T. E.; Buchwald, S. L. *J. Org. Chem.* **2004**, *69*, 5578.
14. Chung, S.; LaMendola, J. *J. Biol. Chem.* **1989**, *264*, 14775.
15. Gui, T.; Tanimoto, T.; Kokai, Y.; Nishimura, C. *Eur. J. Biochem.* **1995**, *227*, 448.
16. *SPARTAN SGI, version 5.1.3 OpenGL*; Wavefunction, Inc.: 18401 Von Karman Avenue, Suite 370, Irvine, CA 92612
17. Alexiou, P.; Nicolaou, I.; Stefek, M.; Kristl, A.; Demopoulos, V. J. *Bioorg. Med. Chem.* **2008**, *16*, 3926.
18. Pegklidou, K.; Koukoulitsa, C.; Nicolaou, I.; Demopoulos, V. J. *Bioorg. Med. Chem.* **2010**, *18*, 2107.
19. Stefek, M.; Snirc, V.; Djoubissie, P. O.; Majekova, M.; Demopoulos, V.; Rackova, L.; Bezakova, Z.; Karasu, C.; Carbone, V.; El-Kabbani, O. *Bioorg. Med. Chem.* **2008**, *16*, 4908.
20. Rees-Milton, K. J.; Jia, Z.; Green, N. C.; Bhatia, M.; El-Kabbani, O.; Flynn, T. G. *Arch. Biochem. Biophys.* **1998**, *355*, 137.
21. Barski, O. A.; Tipparaju, S. M.; Bhatnagar, A. *Drug Metab. Rev.* **2008**, *40*, 553.
22. Srivastava, S. K.; Ramana, K. V.; Bhatnagar, A. *Endocr. Rev.* **2005**, *26*, 380.
23. Cappiello, M.; Voltarelli, M.; Cecconi, I.; Vilardo, P. G.; Dal Monte, M.; Marini, I.; Del Corso, A.; Wilson, D. K.; Quiocho, F. A.; Petrash, J. M.; Mura, U. *J. Biol. Chem.* **1996**, *271*, 33539.
24. Grimshaw, C. E.; Lai, C. J. *Arch. Biochem. Biophys.* **1996**, *327*, 89.
25. Reddy, G. B.; Satyanarayana, A.; Balakrishna, N.; Ayyagari, R.; Padma, M.; Viswanath, K.; Petrash, J. M. *Mol. Vis.* **2008**, *14*, 593.
26. Lee, A. Y.; Chung, S. K.; Chung, S. S. *Proc. Natl. Acad. Sci. U.S.A.* **1995**, *92*, 2780.
27. Terashima, H.; Hama, K.; Yamamoto, R.; Tsuboshima, M.; Kikkawa, R.; Hatanaka, I.; Shigeta, Y. *J. Pharmacol. Exp. Ther.* **1984**, *229*, 226.
28. Das, B.; Srivastava, S. K. *Arch. Biochem. Biophys.* **1985**, *238*, 670.
29. Malone, J. I.; Knox, G.; Benford, S.; Tedesco, T. A. *Diabetes* **1980**, *29*, 861.
30. Schmidt, M.; Michal, M. *Arzneimittelforschung* **1989**, *39*, 493.
31. El-Kabbani, O.; Darmanin, C.; Schneider, T. R.; Hazemann, I.; Ruiz, F.; Oka, M.; Joachimiak, A.; Schulze-Briese, C.; Tomizaki, T.; Mitschler, A.; Podjarny, A. *Proteins* **2004**, *55*, 805.
32. Klebe, G.; Kramer, O.; Sotriffer, C. *Cell. Mol. Life Sci.* **2004**, *61*, 783.
33. El-Kabbani, O.; Carbone, V.; Darmanin, C.; Oka, M.; Mitschler, A.; Podjarny, A.; Schulze-Briese, C.; Chung, R. P. *J. Med. Chem.* **2005**, *48*, 5536.
34. Urzhumtsev, A.; Tete-Favier, F.; Mitschler, A.; Barbanton, J.; Barth, P.; Urzhumtseva, L.; Biellmann, J. F.; Podjarny, A.; Moras, D. *Structure* **1997**, *5*, 601.
35. Koukoulitsa, C.; Zika, C.; Geromichalos, G. D.; Demopoulos, V. J.; Skaltsa, H. *Bioorg. Med. Chem.* **2006**, *14*, 1653.
36. White, J.; McGillivray, G. *J. Org. Chem.* **1977**, *42*, 4248.
37. Costantino, L.; Rastelli, G.; Gamberini, M. C.; Vinson, J. A.; Bose, P.; Iannone, A.; Staffieri, M.; Antolini, L.; Del Corso, A.; Mura, U.; Albasini, A. *J. Med. Chem.* **1999**, *42*, 1881.
38. Rackova, L.; Snirc, V.; Majekova, M.; Majek, P.; Stefek, M. *J. Med. Chem.* **2006**, *49*, 2543.
39. Rackova, L.; Stefek, M.; Majekova, M. *Redox Rep.* **2002**, *7*, 207.
40. Mihaljevic, B.; Katusin-Razem, B.; Razem, D. *Free Radical Biol. Med.* **1996**, *21*, 53.
41. Juskova, M.; Snirc, V.; Krizanova, L.; Stefek, M. *Acta Biochim. Pol.* **2010**, *57*, 153.
42. Mylari, B. L.; Armento, S. J.; Beebe, D. A.; Conn, E. L.; Coutcher, J. B.; Dina, M. S.; O'Gorman, M. T.; Linhares, M. C.; Martin, W. H.; Oates, P. J.; Tess, D. A.; Withbroe, G. J.; Zembrowski, W. J. *J. Med. Chem.* **2003**, *46*, 2283.
43. Carosati, E.; Sciabola, S.; Cruciani, G. *J. Med. Chem.* **2004**, *47*, 5114.
44. GRID version 22, Molecular Discovery Ltd., 4. Chandos Street, W1A 3BQ, London. United Kingdom
45. Goodford, P. J. *J. Med. Chem.* **1985**, *28*, 849.
46. DeLano, W.L. *The PyMOL Molecular Graphics System DeLano Scientific*; San Carlos, CA, USA, 2002